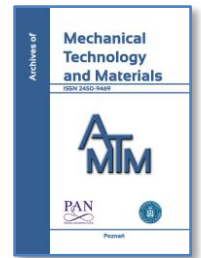


DE GRUYTER  
OPEN

ARCHIVES OF MECHANICAL TECHNOLOGY AND MATERIALS

WWW.AMTM.PUT.POZNAN.PL



# Laser borided composite layer produced on austenitic 316L steel

Daria Mikołajczak <sup>a</sup>, Michał Kulka <sup>a\*</sup>, Natalia Makuch <sup>a</sup>, Piotr Dziarski <sup>a</sup>

<sup>a</sup> Institute of Materials Science and Engineering, Poznan University of Technology

\*Corresponding author, e-mail address: [michal.kulka@put.poznan.pl](mailto:michal.kulka@put.poznan.pl)

## ARTICLE INFO

Received 15 February 2016  
Received in revised form 16 June 2016  
Accepted 22 June 2016

## KEY WORDS

laser boriding,  
austenitic steel,  
microstructure,  
hardness,  
wear resistance

## ABSTRACT

Austenitic 316L steel is well-known for its good resistance to corrosion and oxidation. Therefore, this material is often used wherever corrosive media or high temperatures are to be expected. The main drawback of this material is very low hardness and low resistance to mechanical wear. In this study, the laser boriding was used in order to improve the wear behavior of this material. As a consequence, a composite surface layer was produced. The microstructure of laser-borided steel was characterized by only two zones: re-melted zone and base material. In the re-melted zone, a composite microstructure, consisting of hard ceramic phases (borides) and a soft austenitic matrix, was observed. A significant increase in hardness and wear resistance of such a layer was obtained.

## 1. INTRODUCTION

AISI 316L steel was characterized by an effective balance of chemical composition, i.e. carbon, chromium, nickel and molybdenum concentrations, causing an excellent corrosion resistance. This material was commonly used in aggressive corrosive environments, both at the ambient temperature and at elevated temperature. The relatively low hardness (200 HV) was usually an important disadvantage of this steel. It resulted in its poor wear resistance and was the reason for its limited use. 316L steel could not be subjected to conventional heat treatment because of its austenitic structure. Therefore, there was no easy way to increase wear resistance of this steel [1].

There were attempts to improve tribological properties of the stainless steels using the methods widely applied for constructional or tool steels, such as nitriding, carburizing or boronizing [2-11]. Glow discharge assisted low-temperature nitriding of 316L steel was investigated [2, 3]. This process (at 440°C for 6 h) caused the formation of a thin layer (4 μm) composed of chromium nitrides (CrN) as well as of austenite supersaturated with nitrogen [2]. The increase in process temperature up to 550°C (823 K) resulted in producing the layer of the thickness about 20 μm [3]. Additionally, iron

nitrides (Fe<sub>4</sub>N) were observed in microstructure at higher temperature [3, 4]. The layers also contained Cr<sub>2</sub>N chromium nitrides [5]. Low-temperature plasma carburizing was also applied to improve the properties of stainless steels [6-9]. Such a process, carried out below 520°C (793 K), produced the austenite which was supersaturated with carbon and was characterized by an expanded lattice. Chromium carbides as well as expanded austenite and martensite appeared after carburizing at higher temperature [6]. The thickness of these layers didn't exceed 50 μm. Pack-boronizing was also carried out for austenitic steels [10-12] in the range of temperature 800-950°C, without sacrificing corrosion resistance. The microstructure consisted of two-phase boride layer (FeB + Fe<sub>2</sub>B). After the process at a temperature of 950°C for 8 h, the layer obtained a thickness of 90 μm [10].

Laser modification was well-known as an alternative method for improving the tribological properties. In recent years, laser beam was being used for a wide range of applications in order to modify the microstructure and properties of the metals and their alloys [13, 14]. The most important laser processes were as follows: laser-heat treatment, laser alloying and laser overlaying. Laser boriding of steels [15, 16], nodular cast iron [17], titanium and its alloys [18-21] or Ni-based alloys [22, 23] was also intensively

developed. The hard particles were often introduced to the material surface by the laser treatment. The laser processing might be controlled so as to minimize or promote the dissolution of these particles in the re-melted substrate, leading to a wide variety of metallurgical structures and properties [24]. Laser alloying was applied for 316L stainless steel in order to improve its hardness and wear resistance by incorporating carbides [25] or borides [26].

In this paper, laser boriding of 316L steel was studied as an interesting alternative for diffusion process. The cylindrical surface of the samples was laser-borided with overlapping of 86% like the processes for pure titanium and Inconel 600-alloy previously reported [21-23]. It caused obtaining the uniform laser-borided layer in respect of its thickness, and the laser-borided layer was significantly thicker than that-obtained in case of diffusion boriding. The microstructure, hardness and wear resistance of the produced laser-borided layer were analyzed and discussed.

## 2. EXPERIMENTAL PROCEDURE

AISI 316L austenitic steel was investigated. Its chemical composition was presented in **Table 1**. The ring-shaped specimens (external diameter ca. 20 mm, internal diameter ca. 12 mm and height ca. 12 mm) were used in the study.

**Table 1. Chemical composition of material used [wt pct]**

| Material | C     | Cr    | Ni    | Mo   | Mn   | Si   | Fe      |
|----------|-------|-------|-------|------|------|------|---------|
| 316L     | 0.023 | 17.45 | 12.92 | 2.88 | 0.56 | 0.45 | balance |

The two-step laser alloying process was carried out to produce composite surface layer on 316L steel. The paste, consisting of amorphous boron blended with a diluted polyvinyl alcohol solution, was used as an alloying material. First, the external cylindrical surface of the specimen was coated by this paste. The thickness of paste coating ( $t_c$ ) was equal to 200 or 230  $\mu\text{m}$ . Then, the coated surface was re-melted by the laser beam (**Figure 1**).

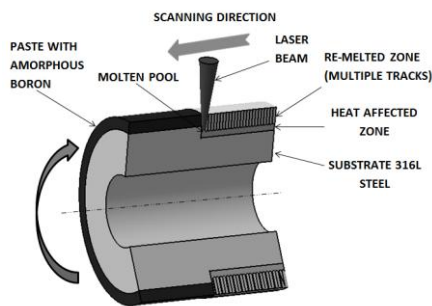


**Fig. 1. The two-step method of laser-boriding**

Laser heat treatment (LHT) was carried out using the TRUMPF TLF 2600 Turbo CO<sub>2</sub> laser of the nominal power 2.6 kW. Laser processing parameters were as follows: laser beam power  $P = 1.82$  kW and scanning rate  $v_f = 2.88$  m/min. The diameter of the laser beam  $d$  was equal to 2 mm. TEM<sub>01\*</sub> multiple mode of the laser beam was applied. Hence, the averaging irradiance ( $E$ ) of about 58 kW/cm<sup>2</sup> was obtained. The focusing mirror was characterized by: curvature 250 mm, diameter 48 mm and focal length 125 mm. The laser

tracks were arranged as multiple tracks (**Figure 2**), with the distance  $f = 0.28$  mm.

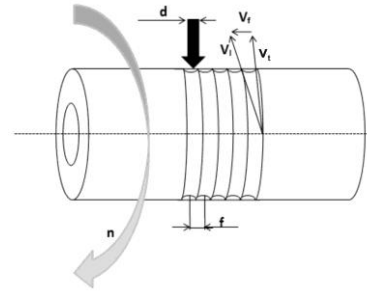


**Fig. 2. Method of multiple tracks producing;**  
 $d$  - laser beam diameter (2 mm);  $v_f$  - rate of feed;  $v_s$  - scanning rate;  $n$  - rotational speed;  $v_t$  - tangential rate;  $f$  - distance from track to track

It corresponded to the distance between the axes of the adjacent tracks and to the feed rate used. The obtained scanning rate  $v_s$  (2.88 m/min) resulted from the rotational speed  $n$  (45.85 min<sup>-1</sup>) and feed rate  $v_f$  (0.28 mm per revolution). Laser processing was realized in argon shielding at a pressure of 0.2 Pa. The relatively high overlapping of the laser tracks (86%) was applied. This value was calculated using the equation as follows:

$$O = \frac{d - f}{d} \cdot 100\% \quad (1)$$

where:  $d$  is a laser beam diameter [mm],  $f$  is the distance between the axes of adjacent tracks [mm], and  $O$  is the overlapping.

The microstructure of polished and etched cross-section of the specimen was observed by an optical microscope (OM) and scanning electron microscope (SEM) Tescan Vega 5135. In order to reveal the microstructure, the etching solution, consisting of anhydrous glycerin, HCl and HNO<sub>3</sub>, was used with a volume ratio of 2:3:1. Phase composition was analyzed using PANalytical EMPYREAN X-ray diffractometer with Cu K $\alpha$  radiation. Microhardness profiles, through the investigated layer, were determined in the polished cross-section of specimen. The Vickers method was applied for microhardness measurements using the apparatus ZWICK 3212 B. The tests were performed under the indentation load of 0.1 kgf (about 0.981 N).

Wear resistance test was applied to evaluate the tribological properties of the produced layer and of the material without treatment. The frictional pair consisted of a cylindrical specimen and a plate-shaped counter-specimen, made of sintered carbide S20S. The scheme of wear was shown in **Figure 3**. The sintered carbide was composed of: 58 wt% of WC, 31.5 wt% of (TiC + TaC + NbC), and 10.5 wt% of Co. Such a material obtained a mass density of 10.7 g/cm<sup>3</sup> and hardness of 1430 HV. The wear tests were conducted under conditions of dry friction (unlubricated sliding contact) using the load  $P = 49$  N and the specimen speed of 0.26 m/s, resulting from the rotational speed  $n=250$  min<sup>-1</sup> and the external diameter of the specimen (20 mm). The laser treatment caused a change in surface roughness of the sample, which was not specially prepared before the wear test. Wear resistance was evaluated by relative mass loss of

specimen and counter-specimen ( $\Delta m/m_i$ ) according to the equation:

$$\frac{\Delta m}{m_i} = \frac{m_i - m_f}{m_i} \quad (2)$$

where:  $\Delta m$  is mass loss [mg],  $m_i$  is initial mass of specimen or counterspecimen [mg],  $m_f$  is final mass of specimen or counterspecimen [mg].

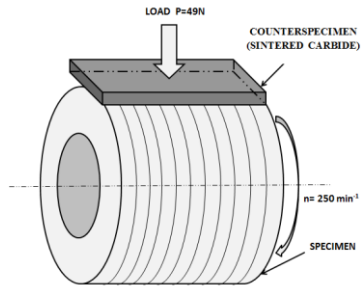


Fig. 3. Scheme of wear test.  $P = 49 \text{ N}$ , rotational speed  $n=250 \text{ min}^{-1}$

### 3. RESULTS AND DISCUSSION

#### 3.1. Microstructure

OM microstructures of laser-alloyed 316L steel using boron as alloying material were shown in **Figure 4**.

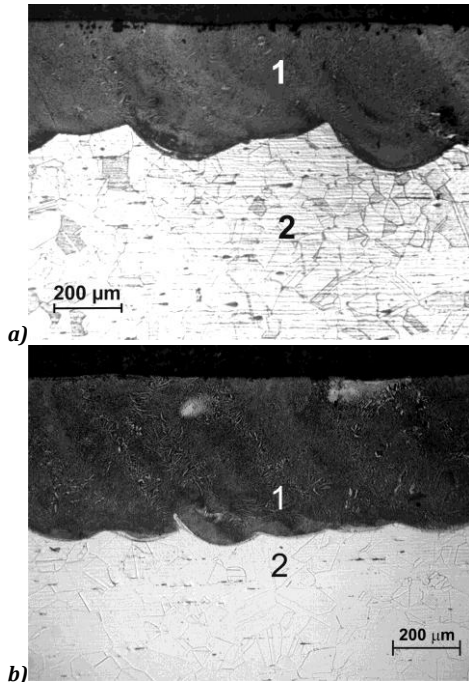


Fig. 4. Microstructure of laser-borided 316L steel at laser beam power of 1.82 kW using paste coating with thickness: 230  $\mu\text{m}$  (a) and 200  $\mu\text{m}$  (b); 1 - remelted zone (MZ); 2 - substrate

The laser treatment was carried out at laser beam power of 1.82 kW using the two thicknesses of paste coating with boron (200 and 230  $\mu\text{m}$ ). The continuous laser-borided layer

was obtained at the surface. Two zones were visible in the microstructure: MZ - laser re-melted zone (1) and the substrate (2). There were no changes in microstructure below MZ, and heat-affected zone (HAZ) was invisible. The reason for such a situation was that an austenitic structure of 316L steel could not be quenched, irrespective of cooling rate obtained during LHT. The microcracks as well as gas pores were not detected in the laser-alloyed layer. The use of thinner paste coating with boron (200  $\mu\text{m}$ ) resulted in higher depth of MZ and more uniform layer in respect of the thickness (**Figure 4b**).

Literature data [10-12] reported the presence of iron borides ( $\text{Fe}_2\text{B}$  and  $\text{Fe}_2\text{B}_3$ ) after diffusion boriding of austenitic steel. After laser boriding,  $\text{Fe}_2\text{B}$ ,  $\text{Cr}_2\text{B}$  and  $\text{Ni}_2\text{B}$  borides were identified in MZ based on the obtained XRD patterns (**Figure 5**).

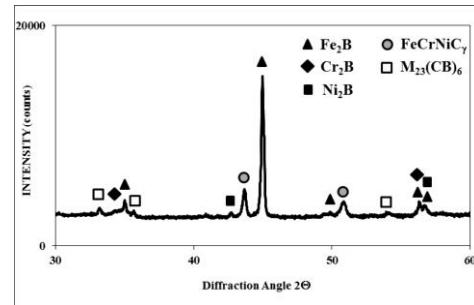


Fig. 5. XRD patterns of laser-borided 316L steel

Additionally, the FeCrNi austenite and borocarbides  $\text{M}_{23}(\text{C,B})_6$  were observed in this zone. Hence, the laser alloying with boron caused the formation of a composite layer. SE image of MZ indicated the presence of composite microstructure, consisting of hard ceramic phases (iron, chromium and nickel borides) and soft austenitic matrix (**Figure 6**). It was previously observed for laser-fabricated Fe-Ni-Co-Cr-B austenitic alloy on 316L steel [24].

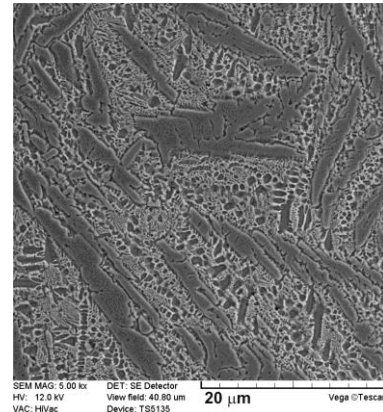


Fig. 6. SE image of re-melted zone (MZ). Hard ceramic phases (iron and chromium borides) in a soft austenitic matrix

#### 3.2. Microhardness profiles

The microhardness profiles of laser-borided layers produced on austenitic 316L steel were shown in **Figure 7**. The measurements were performed perpendicular to the laser-alloyed surface along the axis of laser track as well as along the contact of adjacent tracks. In **Figure 7a**, the

microhardness profiles along the axis of track were compared for two used thicknesses of paste coating (200 and 230  $\mu\text{m}$ ). The use of thicker paste coating with boron (230  $\mu\text{m}$ ) resulted in smaller depth of hardened re-melted zone (MZ). It was accompanied by higher hardness of this zone (up to 740 HV). The higher percentage of hard borides in austenitic matrix was the reason for such a situation. In case of thinner paste coating with boron (200  $\mu\text{m}$ ), the maximal hardness of MZ obtained about 600 HV. Hardness of MZ gradually decreased at the end of MZ because of the diminished percentage of borides, obtaining finally the hardness of the base material (160-190 HV). The slightly smaller depth of MZ was also observed at the contact of adjacent tracks (Figure 7b). However, the hardness of MZ was very similar, irrespective of the place of measurements (along the axis of laser track or along the contact of tracks).

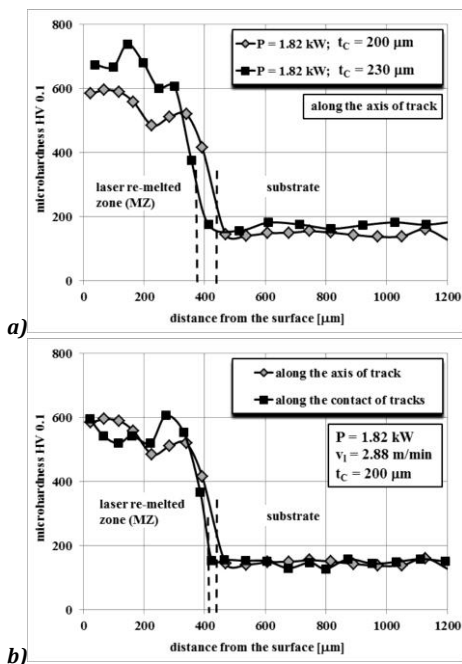


Fig. 7. Microhardness profiles of laser-borided layer formed on 316L steel: along the axis of track at various thickness of paste coating  $t_c$  (a), at the thickness of paste coating  $t_c = 200 \mu\text{m}$ , depending on the measurement place (b)

### 3.3. Wear tests

Wear resistance test was performed for laser-alloyed layer obtained with the use of thinner paste coating with boron (200  $\mu\text{m}$ ). Specimen was investigated for one hour with a change in the counter-specimen (sintered carbide) every half an hour. The results were compared to those obtained for 316L steel without treatment [25] and were presented in Figure 8.

The evaluation using relative mass loss of specimen and counter-specimen  $\Delta m/m_i$  indicated the significant increase in wear resistance of laser-borided layer in comparison with untreated 316L steel. The specimen with the produced layer was characterized by the considerably lower relative mass loss than that obtained in case of austenitic steel without treatment. The wear of counter-specimen (sintered carbide S20S) was very small in comparison with the examined samples.

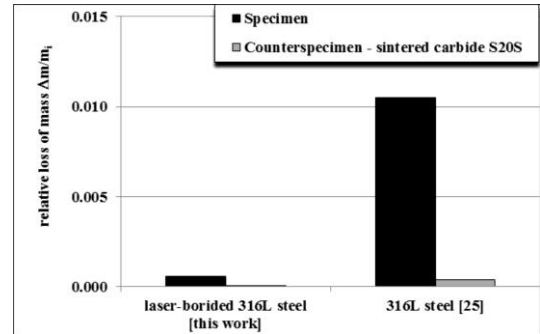


Fig. 8. The results of wear resistance tests

## 4. CONCLUSIONS

Laser alloying with boron was applied in order to produce composite surface layers on austenitic 316L steel. The microstructure was characterized by only two zones: laser re-melted zone (MZ) and the substrate. There were no visible effects of heat treatment below MZ in microstructure. Heat-affected zone was not observed because austenitic steel could not be hardened by typical heat treatment (austenitizing and quenching). The composite microstructure of MZ consisted of hard ceramic phases (iron, chromium and nickel borides) with a soft austenitic matrix. The uniform laser-alloyed layers in respect of the thickness were produced because of the relatively high overlapping of multiple laser tracks (86%). Cracks and gas pores were not observed.

The significant increase in hardness was characteristic of produced surface layers. Hardness of MZ obtained 600 HV and 740 HV, depending on the thickness of paste coating with boron. At the end of MZ, hardness gradually decreased to the values characteristic of the substrate (160-190 HV) because of the increased percentage of soft austenitic matrix. The use of thinner paste coating with boron resulted in higher depth of re-melted zone. It was accompanied by diminished hardness because of the lower percentage of hard borides in austenitic matrix.

Laser alloying with boron caused also a significant increase in wear resistance. Relative mass loss of laser-borided specimen was approximately ten times lower than that measured for austenitic 316L steel without treatment.

The applications of proposed layers in industry will require the appropriate corrosion resistance. It should be examined in the future and should be compared to the properties of 316L steel without surface layer.

## REFERENCES

- [1] Glaeser W.A., Materials for Tribology, Tribology Series, 20, Elsevier, 1992.
- [2] Skołek-Stefaniszyn E., Kaminski J., Sobczak J., Wierzchoń T., Modifying the properties of AISI 316L steel by glow discharge assisted low-temperature nitriding and oxynitriding, Vacuum 85 (2010) 164-169.
- [3] Skołek-Stefaniszyn E., Burdyska S., Mroz W., Wierzchoń T., Structure and wear resistance of the composite layers produced by glow discharge nitriding and PLD method on AISI 316L austenitic stainless steel, Vacuum 83 (2009) 1442-1447.
- [4] Li Y., Wang Z., Wang L., Surface properties of nitrided layer on AISI 316L austenitic stainless steel produced by high

- temperature plasma nitriding in short time, *Applied Surface Science* 298 (2014) 243-250.
- [5] **Fraćzek T., Olejnik M., Jasiński J., Skuza Z.**, Short-term low-temperature glow discharge nitriding of 361L austenitic steel, *Metallurgija* 50 (3) (2011) 151-154.
- [6] **Sun Y., Li X., Bell T.**, Structural characteristics of low temperature plasma carburised austenitic stainless steel, *Materials Science and Technology* 15 (1999) 1171-1178.
- [7] **García Molleja J., Nosei L., Ferrón J., Bemporad E., Lesage J., Chicot D., Feugeas J.**, Characterization of expanded austenite developed on AISI 316L stainless steel by plasma carburization, *Surface and Coatings Technology* 204 (2010) 3750-3759.
- [8] **Ceschini L., Chiavari C., Lanzoni E., Martini C.**, Low-temperature carburised AISI 316L austenitic stainless steel: Wear and corrosion behavior, *Materials and Design* 38 (2012) 154-160.
- [9] **Sun Y.**, Tribocorrosion behavior of low temperature plasma carburized stainless steel, *Surface and Coatings Technology* 228 (2013) S342-S348.
- [10] **Ozdemir O., Omar M.A., Usta M., Zeytin S., Bindal C., Ucisik A.H.**, An investigation on boriding kinetics of AISI 316 stainless steel, *Vacuum* 83 (2009) 175-179.
- [11] **Balusamy T., Sankara Narayanan T.S.N., Ravichandran K., Park I.S., Lee M.H.**, Effect of surface mechanical attrition treatment (SMAT) on pack boronizing of AISI 304 stainless steel, *Surface & Coatings Technology* 232 (2013) 60-67.
- [12] **Kayali Y., Büyüksagis A., Yalçin Y.**, Corrosion and Wear Behaviors of Boronized AISI 316L Stainless Steel, *Metals and Materials International* 19 (5) (2013) 1053-1061.
- [13] **Major B.**, Chapter 7: Laser processing for surface modification by remelting and alloying of metallic systems in "Materials Surface Processing by Directed Energy Techniques" Edited by Yves Paleau, Elsevier (2006).
- [14] **Goły M., Kusiński J.**, Microstructure and properties of the laser treated 30CrMnMo16-8 chromium steel, in: Problems of modern techniques in aspect of engineering and education, eds.: Paweł Kurtyka [et al.], Monography, Pedagogical University. Cracow. Institute of Technology (2006) 183-188.
- [15] **Bartkowiak K., Waligóra W.**, Laser alloying of the construction steel 45 with boron. The scientific conference with foreign participation, TRANSFER 2001, Trenčín, Slovak Republic, 23-24 October 2001, 175-180.
- [16] **Kulka M., Makuch N., Pertek A.**, Microstructure and properties of laser-borided 41Cr4 steel. *Optics & Laser Technology* 45 (2013) 308-318.
- [17] **Paczkowska M., Ratuszek W., Waligóra W.**, Microstructure of laser boronized nodular iron. *Surf. Coat. Technol.* 205 (2010) 2542-2545.
- [18] **Filip R., Sieniawski J., Pleszakow E.**, Formation of surface layers on Ti-6Al-4V titanium alloy by laser alloying. *Surf. Eng.* 22(1) (2006) 53-57.
- [19] **Tian Y.S., Zhang Q.Y., Wang D.Y.**, Study on the microstructures and properties of the boride layers laser fabricated on Ti-6Al-4V alloy. *J. Mater. Process. Technol.* 209 (2009) 2887-2891.
- [20] **Guo C., Zhou J., Zhao J., Guo B., Yu Y., Zhou H., Chen J.**, Microstructure and friction and wear behavior of laser boronizing composite coatings on titanium substrate. *Appl. Surf. Sci.* 257 (2011) 4398-4405.
- [21] **Kulka M., Makuch N., Dziarski P., Piasecki A., Miklaszewski A.**, Microstructure and properties of laser-borided composite layers formed on commercially pure titanium, *Optics and Laser Technology* 56 (2014) 409-424.
- [22] **Kulka M., Dziarski P., Makuch N., Piasecki A., Miklaszewski A.**, Microstructure and properties of laser-borided Inconel 600-alloy, *Applied Surface Science* 284 (2013) 757-771.
- [23] **Kulka M., Makuch N., Dziarski P., Piasecki A.**, A study of nanoindentation for mechanical characterization of chromium and nickel borides' mixtures formed by laser boriding, *Ceramics International* 40(4) (2014) 6083-6094.
- [24] **Kwok C.T., Cheng F.T., Man H.C.**, Laser-fabricated Fe-Ni-Co-Cr-B austenitic alloy on steels. Part I. Microstructures and cavitation erosion behavior, *Surface and Coatings Technology* 145 (2001) 194-205.
- [25] **Kim T.H., Kim B.C.**, Chromium carbide laser-beam surface-alloying treatment on stainless steel, *Journal of Materials Science* 27 (1992) 2967-2973.
- [26] **Kulka M., Mikołajczak D., Makuch N., Dziarski P.**, Laser alloying of 316L steel with boron, *Inżynieria Materiałowa* 6 (2014) 512-515.